Stress redistributions in unit cells of fibre-reinforced polymer composites with interface degradation

Luis A. Godoy*

Structures Department, FCEFyN,
Universidad Nacional de Córdoba,
P.O. Box 916, Córdoba 5000, and CONICET, Argentina
E-mail: lgodoy@com.uncor.edu
*Corresponding author

Victoria Mondragón

Diseño y Construcción de Obras Civiles JMT,
Bogotá, Colombia
E-mail: victoriam@jamesmayorcatorres.com

Miguel A. Pando

Department of Civil and Environmental Engineering,
University of North Carolina at Charlotte,
Charlotte, NC 28223, USA
E-mail: mpando@uncc.edu

Felipe J. Acosta

Department of Civil Engineering and Surveying,
University of Puerto Rico at Mayagüez,
Mayagüez, PR 00680, Puerto Rico
E-mail: felipe.acosta1@upr.edu

Abstract: Experimental evidence indicates that the main damage mechanisms found in fibre-reinforced composites under static loading or environmental action are matrix damage, fibre damage and interface damage, leading to various forms of strong inhomogeneities at the micromechanical level. The main objective of this paper is to identify the stress redistributions that take place at the unit cell level, in which damage has already occurred due to an independent process. A deterministic approach is carried out to illustrate the main features of the transverse behaviour of a unidirectional fibre-reinforced composite under static loading. Damage is modelled by means of interface defects, in which the number and size of defects are considered as parameters of the damaged configuration and also by changes in material properties. The two-dimensional problem is solved using a general purpose finite-element code. The results show the extent of damage propagation to be expected in several configurations with inhomogeneities.

Copyright © 2013 Inderscience Enterprises Ltd.

Keywords: fibre-reinforced polymer composites; finite elements; interface degradation; stresses; unit cell analysis.

Reference to this paper should be made as follows: Godoy, L.A., Mondragón, V., Pando, M.A. and Acosta, F.J. (2013) 'Stress redistributions in unit cells of fibre-reinforced polymer composites with interface degradation', *Int. J. Microstructure and Materials Properties*, Vol. 8, No. 3, pp.185–206.

Biographical notes: Luis A. Godoy holds a PhD in Civil Engineering from the University of London (1979). His areas of research include applied and theoretical mechanics, elastic stability and thin walled structures. He is a member of the American Society of Civil Engineers, the American Society of Engineering Education and several other professional associations. Currently, he is a Senior Full Professor in the Structures Department of the National University of Cordoba in Argentina, and Principal Researcher of the Science Research Council of Argentina (CONICET).

Victoria Mondragón obtained her BSc in Civil Engineering from the University of El Valle, in Cali, Colombia and an MS in Civil Engineering (Structural Engineering concentration, 2008). She is currently a Consulting Engineering in Structural Engineering in Bogota, Colombia.

Miguel A. Pando received his BS, MS and PhD degrees from the Javeriana University, the University of Alberta and Virginia Tech, respectively. He has several publications, including his PhD dissertation, related to FRP composite pile foundations in marine environments. He is a member of the American Society of Civil Engineers, the Transportation Research Board and several other professional associations. His research interests include use of composite materials in civil engineering applications, soil-structure interaction, and characterisation of geomaterials. Currently, he is an Associate Professor at the University of North Carolina at Charlotte in Charlotte, NC, USA.

Felipe J. Acosta is a Professor of the Department of Civil Engineering and Surveying of the University of Puerto Rico at Mayaguez. He is also the Director of the Department's Construction Materials Laboratory. He obtained his PhD from Georgia Institute of Technology, Atlanta, GA, USA, in 1999. He is a Professional Engineer registered in Puerto Rico. In the summers of 2003, 2004 and 2006 he participated in the NASA Summer Faculty Fellowship program. His areas of expertise are mechanical behaviour of composite materials, finite-element analysis, mechanics of composite materials and the uses of recycled materials in construction applications.

1 Introduction

The degradation of mechanical properties in Glass Fibre-Reinforced Polymers (GFRP) due to moisture and temperature effects is of crucial importance for the design and the durability assessment of a composite material. Such degradation is usually known as ageing, because moisture diffusion, UV and other environmental actions can produce high levels of damage at the micromechanics level as a function of time. Some of the moisture-induced degradation has been found to be reversible and some is irreversible, as independently shown by Shutte (1994), Zhang et al. (2003) and Helbling and Karbhari (2005).

A number of ageing processes under controlled conditions followed by coupon testing have been reported in the literature. Kajorncheappunngam et al. (2002) tested that GFRP composite coupons immersed up to five months in four different liquids and two main temperatures (20°C and 60°C) to induce ageing. The specific material tested was E-GFRP with epoxy resin. Similar results and trends had been previously reported by Davies et al. (1996).

The current available experimental evidence is not sufficient to predict how this local moisture induces fibre and matrix irreversible damage, but observations indicate that the most common damage mechanism involves small voids at the fibre–matrix interface and depending on polymer matrix type and properties, matrix damage can also occur. The extent of this damage of a GFRP submerged at either ambient or elevated temperature, is also a function of the specific liquid in which the composite is immersed. Interface damage has been reported by Cervenka et al. (2004) in composites immersed in water vapour. Damage mechanisms have also been considered by Foulc et al. (2005), who identified the occurrence of plasticity, chemical degradation, morphological evolution and interface damage with debonding. In summary, the main damage mechanisms found in GFRP composites under static loading and exposed to environmental action, such as water or ultra violet (UV) radiation, are damage to the resin matrix in the form of microcracks, to the fibre or to the interface including localised debonding.

Various forms of strong inhomogeneities may exist at the micromechanical level, which have traditionally been computationally modelled by means of degradation of the constituent properties and/or by inclusion of a finite set of defects in the composite constituents or at their interface.

A classical approach to represent the consequences of damage is the use of Damage Mechanics, a theory originally developed in the 1950s by Kachanov (1986) and further explored by a number of researchers (see for example, Lemaitre and Krajcinovic, 1988; Lemaitre and Desmorat, 2010). Under this approach, damage in the composite material is assumed in the form of voids and considers average values of effective sections. This methodology does not provide information about the behaviour at the micro level.

An alternative approach is to obtain the local properties including damage from a detailed analysis at the micro level. The main assumption employed to carry out a micromechanical analysis of materials with periodic structure is that the local microstructure may be represented by a small volume (Representative Volume Element, RVE) or a Unit Cell (UC). Such reduced domain may include a single fibre or several fibres, depending on the symmetry of the material configuration under consideration.

The most common approach to couple the micro-information to a macro scale is homogenisation (Sanchez-Palencia and Zaoui, 1987), in which a heterogeneous RVE is defined and is assumed to be equivalent to a homogeneous media in the macro problem. This procedure requires the solution of a cell problem using periodic boundary conditions.

Several researchers have investigated damage in composites due to loading, rather than ageing. Thus, damage is not present at the initial stages of the study, but it develops as a consequence of the loads being applied to the composite and transferred to a UC. For example Hutchinson and co-workers have investigated the development of inelastic strains associated to matrix cracking in ceramic composites (e.g., He et al., 1994;

Budiansky et al., 1995). More recently, Bonora and Ruggiero (2005) also studied that damage mechanics in composites by considering several configurations of UC using finite elements, and they found that the stress–strain curve has three distinct parts: a linear elastic behaviour; a change in the slope with separation between matrix and fibre and a rapid increase in strains accompanied by cracking for small stress increments. A similar approach was followed by Caporale et al. (2006) to emphasise interface failure by use of elasto-fragile springs. Car et al. (2002) focused on the scale coupling in composites. In all cases, two-dimensional domains were assumed in order to work with simple mesh domains.

To understand the micromechanical behaviour of the damaged material, it is necessary to identify the stress redistributions that take place at the UC level, in which damage has already occurred due to an independent process. Such situation is a typical of ageing processes, in which severe degradation may have been taken place due to the environmental action before loads are applied to the structural component. One of the most complete studies on the mechanical behaviour of a unit cell having defects or damage before the application of loads was published by Kaminski (2005). This researcher considered that the computational modelling of composite materials at the micro level using finite elements to represent the influence of local damage in 1/4 of a UC. Kaminski was not concerned with the source of damage, and produced models of damage using voids at the fibre/matrix interface for unit cells. First, he assumed that a finite number of defects were present in the material in all composite interfaces. Since defects are here introduced at the UC level, then it is assumed that this damage is also present in all fibres in a given neighbourhood. Second, each defect is assumed as a bubble having a characteristic radius. Although in real situations the shape of a bubble may be irregular, Kaminski assumed a semi-circular void. Third, this bubble radius is assumed to be small with respect to the domain considered. To introduce the randomness in the analysis, Kaminski adopted random parameters to characterise the total number of defects at an interface and their radii. Fibre damage was also modelled with voids penetrating the fibre. Such voids penetrating the fibre have the shape of a teeth with their sharp sides directed towards the centre of the fibre. Plane strain domains were investigated using some 300 finite elements to represent 1/4 of the UC. According to the author, “the model introduced approximates the real defects rather precisely” (Kaminski, 2005, p.37).

In summary, most previous studies on damage of composites at the micro level employ a two-dimensional domain at a UC level (rather than RVE), in which defects are modelled by means of semi-circular bubbles or voids.

The present work considers the transverse behaviour of damaged unit cells, involving stress redistributions of a GFRP composite under static loading. The modelling presented is deterministic and uses a plane strain representation of a unit cell. Damage or degradation is represented by means of interface defects, in which the number and size of defects are considered as parameters of the damaged configuration. The actual mechanism of initiation of damage, for example due to moisture diffusion or its progress due to mechanical loads, is not modelled so that the passage from a ‘perfect’ configuration to a ‘damaged’ one would be represented by phenomenological laws derived from experiments.

2 Illustrative evidence of macroscopic damage due to ageing

Perhaps the elastic modulus and the tensile strength at the macro structural level are the most commonly reported features in the literature on the mechanical consequences of hygro-thermal ageing in GFRP composites.

A summary of the results obtained by Kajorncheappunngam et al. (2002) for tensile strength and stiffness are shown in Figure 1(a) and (b), respectively. These results are for distilled and salt water. To facilitate the visualisation of the degradation effects, the vertical axis in both plots has been normalised with respect to the values of tensile strength and elastic modulus at the initial time (i.e., unaged specimens); those are indicated in Figure 1 as 'Normalised Failure Stress' and 'Normalised Modulus' respectively. For this study, the average tensile strength of unaged specimens was 400 MPa, and the stiffness or elastic modulus at the initial time was 21 GPa. The results reported in Kajorncheappunngam et al. (2002) indicated that there are only small changes in the elastic modulus, but the more significant changes occur in the strength of the composite.

Figure 1 Influence of aging on (a) tensile strength; (b) modulus of elasticity (see online version for colours)

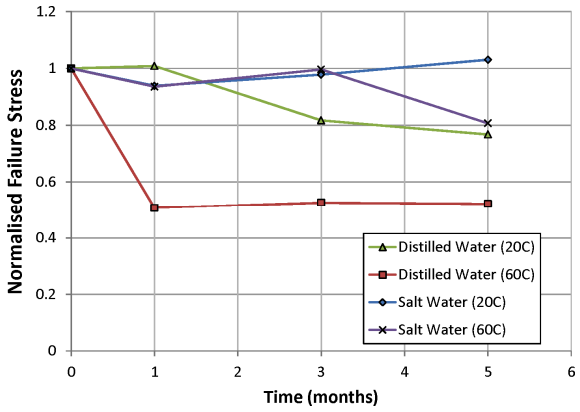

(a)

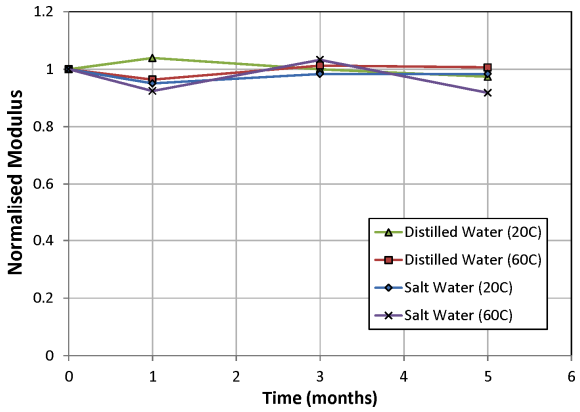

(b)

Source: Adapted from Kajorncheappunngam et al. (2002)

3 Illustrative evidence of microscopic damage due to ageing

To illustrate the type of damage that occurs in GFRP composites due to immersion in water, a case tested as part of this research is discussed in this section. Uni-directional GFRP composites with Fibre Volume Fraction $V_f = 0.48$ were tested under axial tension before and after ageing. Tension tests were carried out using an Instron test frame operated at a constant rate of displacement of 1.27 mm/min and the test setup and procedure were performed in general accordance with ASTM Test Method for Tensile Properties of Polymer Matrix Composite Materials (D3039) (ASTM, 2008).

Before ageing, the average tensile strength of epoxy coupons was found to be 47.36 MPa, the average tensile strength of the unidirectional GFRP composite was 60.91 MPa, and the shear strength was half of that, i.e., 30.45 MPa (these results are average values based on the four tests). Accelerated ageing of epoxy and GFRP coupons was achieved by immersion in distilled water at 70°C, a temperature below the curing temperature of the epoxy (80°C) so that the chemical properties of the composite were not modified. After a 90 days immersion period, the average gravimetric moisture content of the GFRP coupons was 0.28.

To visualise damage due to this hygro-thermal ageing, samples were carefully cut using a diamond saw and the surface to be investigated was polished and prepared using standard techniques for Scanning Electron Microscopy (SEM). Figure 2 shows four SEM images with magnification values between 2000X and 3500X. Although the average V_f of the GFRP coupon is 0.48, the SEM images show local variations of fibre volume fractions. The higher V_f values correspond to zones inside the fibre rovings. Using the image analysis, the V_f of each image was 0.94, 0.79, 0.63 and 0.48 for the images shown in Figure 2(a)–(d), respectively. In all cases, damage was observed in the SEM images, and confirmed with optical microscopy, at the fibre–matrix interface. To quantify the level of damage, the image analysis included measurement of the circumferential length of the damaged zone and this measurement was compared with the perimeter of all fibres (or fractions of fibres) present in each image. For example, two fibres showed damage in Figure 1(a). Damage values of 16, 17, 21 and 19% were measured from Figure 1(a)–(d), respectively. As a reference value, McBagonluri et al. (2000) used a similar procedure and found 18% damage on the GFR composites after an 18-day immersion in fresh water at 65°C.

Figure 2 SEM images of E-GFRP unidirectional composite after nine days of immersion in distilled water at 70°C at four locations: (a) Location 1; (b) Location 2; (c) Location 3 and (d) Location 4

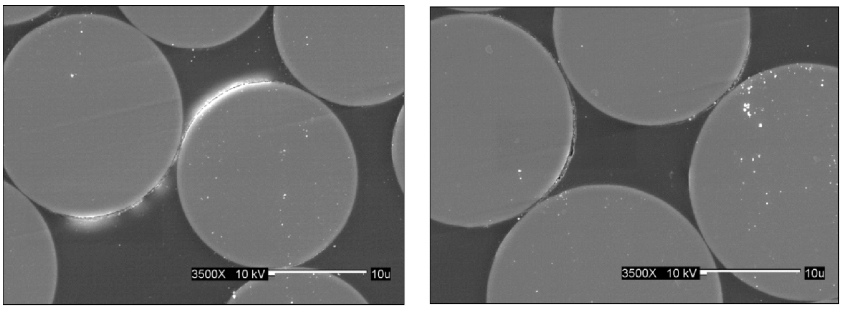

(a) (b)

Figure 2 SEM images of E-GFRP unidirectional composite after nine days of immersion in distilled water at 70°C at four locations: (a) Location 1; (b) Location 2; (c) Location 3 and (d) Location 4 (continued)

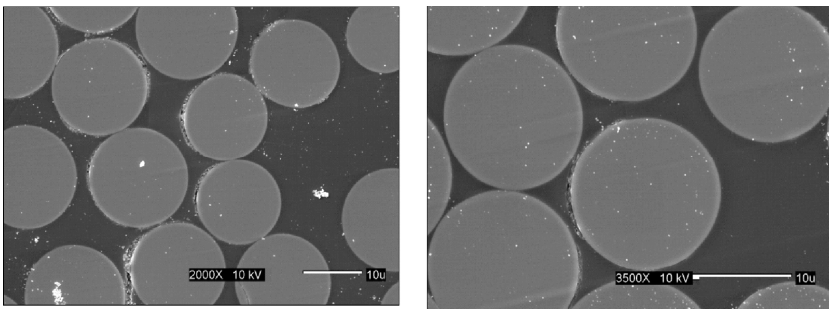

(c) (d)

The observations reported are only indicative of the localisation and possible distribution of damage in a small RVE. A possible way to model the interface damage shown in this section is by specifying interface voids. The specific form of the void is not simple to establish from the limited observations available, but they seem to conform to an elliptical void with a large aspect ratio between the two ellipse diameters.

4 Elastic stress redistributions in unit cells (UC) with interface damage

Interest in understanding the behaviour of the material at the micro level can be manyfold: to visualise the consequences of material degradation (such as degradation due to exposure to hygro-thermal conditions) on the stress response; to obtain equivalent properties of the micro domain and to develop sound basis on which a macro–micro coupling can be built using homogenisation theory. The word redistribution is here used to denote changes in stresses with respect to the stresses present in the undamaged state.

Two scales of analysis were used in this research: one scale considers a UC in which damage around a void is represented, as shown in Figure 3. The other scale considered focuses its attention on the stress redistributions at the local area around a void.

Figure 3 Description of the basic unit cell for the finite element model: (a) unit biaxial load and (b) unit shear load (see online version for colours)

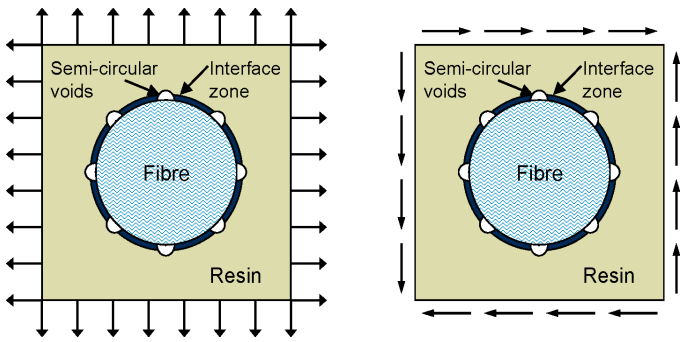

(a) (b)

4.1 Elastic stresses around a fibre in a UC

GFRP modelling at the micro level was performed in this research in order to understand the main features of the behaviour due to damage. Based on the evidence from hygro-thermal ageing reported in the literature, damage was represented in the models by voids located at the interface between the fibre and the surrounding epoxy. The loading conditions at the boundaries of the UC were assumed to be representative of the components of the stress tensor in the macro problem, and periodicity was assumed so that the behaviour of a UC was considered to be similar to the behaviour of all other UC in the neighbourhood. The size of a UC is fixed by the separation between fibres in a composite.

Because of the presence of a defect, it was anticipated that significant redistributions of stresses would occur inside the UC domain; thus, the first stage was to understand the level of elastic stress redistributions that would take place for several defect conditions, including the influence of the number and size of the defects assumed at the interface.

The values adopted for properties of constituent materials was based on the Barbero (2010) as follows: modulus of elasticity 84,000 MPa for the E-glass fibre and 4000 MPa for the epoxy resin, whereas Poisson's ratios were 0.22 and 0.38, respectively. It was assumed that plasticity in the epoxy started at a value of 48.26 MPa. The fibre diameter was 7 μm in all cases.

The finite-element package ABAQUS was used to model the UC. Simple three-node, plane strain, triangular finite elements were used, so that it was necessary to employ dense meshes of elements (see example shown in Figure 4) to cover areas of high-stress gradients. To reach convergence in zones of stress concentrations, approximately 350,000 elements (or 180,000 nodes) were used in most discretisations of a unit cell containing damage. A complete fibre was included in the analyses (instead of 1/4, as considered by other authors) to be able to represent shear loads and non-symmetric configurations, as shown in Figure 3(b).

Figure 4 Finite element mesh of the unit cell with discrete damage (see online version for colours)

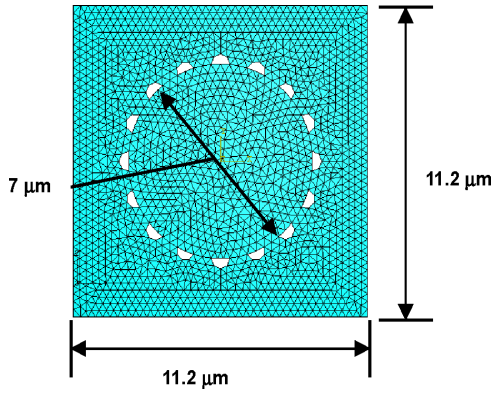

First, the influence of a fixed-size semi-circular void with a diameter equal to 10% the diameter of the fibre was investigated in configurations of 4, 8 and 16 symmetric voids around the interface. For a biaxial stress field of unit value, the configurations of 4 and 8 voids did not show interactions and each void could be considered as a case

of stress concentration. Only for 16 voids (in which case two contiguous voids are approximately separated one void diameter from each other) there is interaction in the stress field, as shown in Figure 5. The same situation occurred for shear loads (Figure 6).

Figure 5 Elastic stress redistribution under unit biaxial load. von Mises stress for (a) 8 semicircular voids and (b) 16 semicircular voids (see online version for colours)

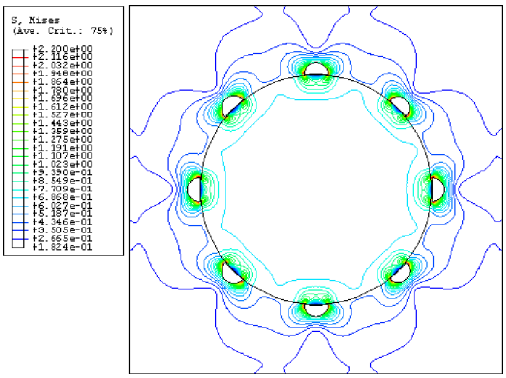

(a)

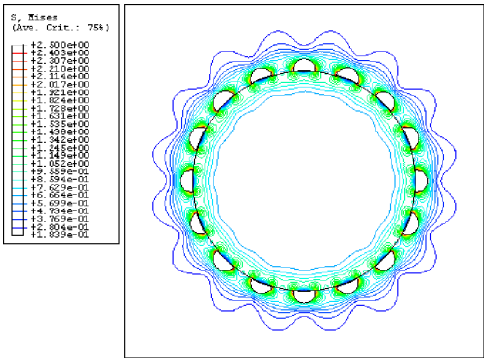

(b)

Figure 6 Elastic stress redistribution under unit shear load. von Mises stress for (a) 8 semicircular voids and (b) 16 semicircular voids (see online version for colours)

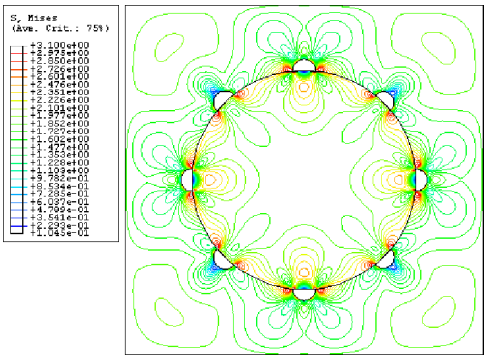

(a)

Figure 6 Elastic stress redistribution under unit shear load. von Mises stress for (a) 8 semicircular voids and (b) 16 semicircular voids (see online version for colours) (continued)

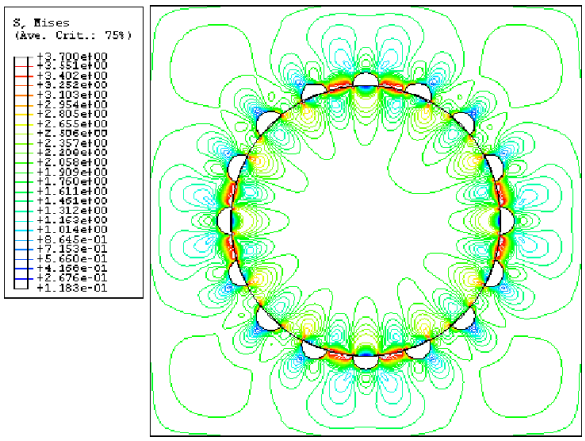

(b)

The influence of void size was studied for void diameters ranging from 10% to 25% of the fibre diameter. For the larger voids the separation was 2.14 times the diameter of a void. Under biaxial loading, the increase in void diameter resulted in an increase in the von Mises stresses, as shown in Figure 7. In comparison with the case of smaller void equal to 10% the fibre diameter, an 8% increase in von Mises stress was detected for void diameter equal to 15% the fibre diameter; 22% for the 20% diameter; and 33% for the 25% diameter. For the case of unit shear load, shown in Figure 8, the increases in von Mises stresses σ_e were of 4%, 13% and 25% for the void sizes of 15%, 20% and 25% of the fibre diameter, respectively.

Figure 7 Elastic stress redistribution under unit biaxial load. von Mises stress for void diameter equal to (a) 20% fibre diameter and (b) 25% fibre diameter (see online version for colours)

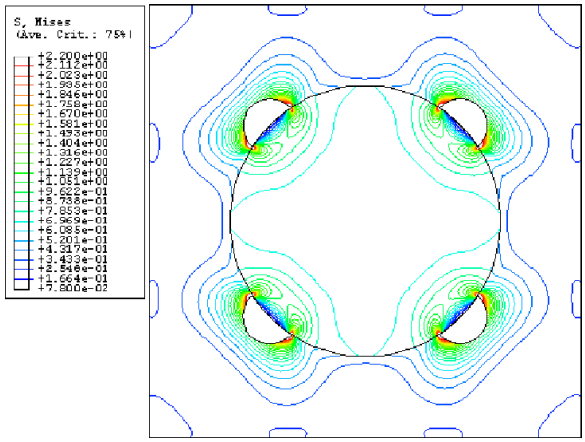

(a)

Figure 7 Elastic stress redistribution under unit biaxial load. von Mises stress for void diameter equal to (a) 20% fibre diameter and (b) 25% fibre diameter (see online version for colours) (continued)

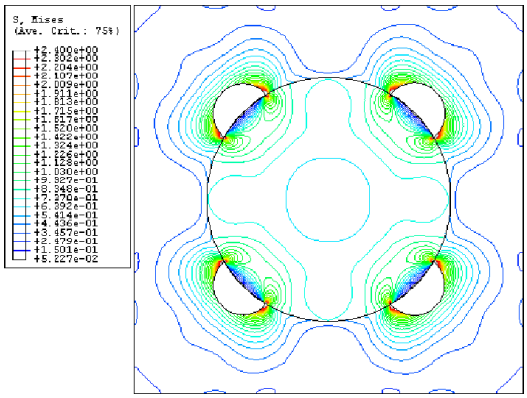

(b)

Figure 8 Elastic stress redistribution under unit shear load. Von Mises stress for void diameter equal to (a) 20% fibre diameter and (b) 25% fibre diameter (see online version for colours)

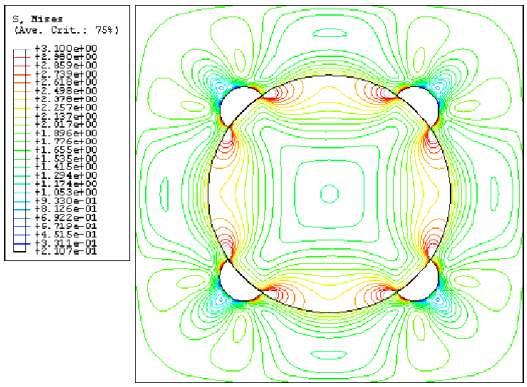

(a)

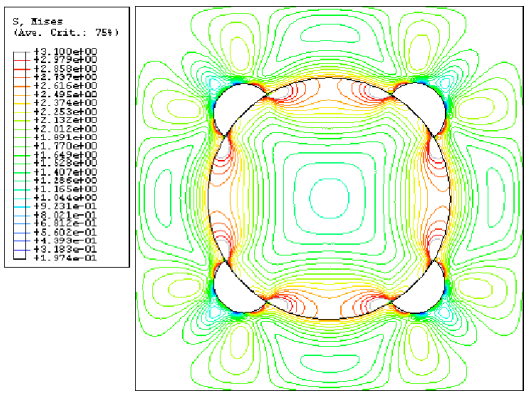

(b)

Regarding the elastic parameters as measured at a UC level, the results are plotted in Figure 9 for increasing number of voids and in Figure 10 for increasing void diameter. In both cases, it may be seen that there are no significant changes in the transverse elastic modulus E_2 or in the shear modulus G_{12} of the GFRP composite.

Figure 9 Sensitivity of elastic modulus with number of voids at UC level

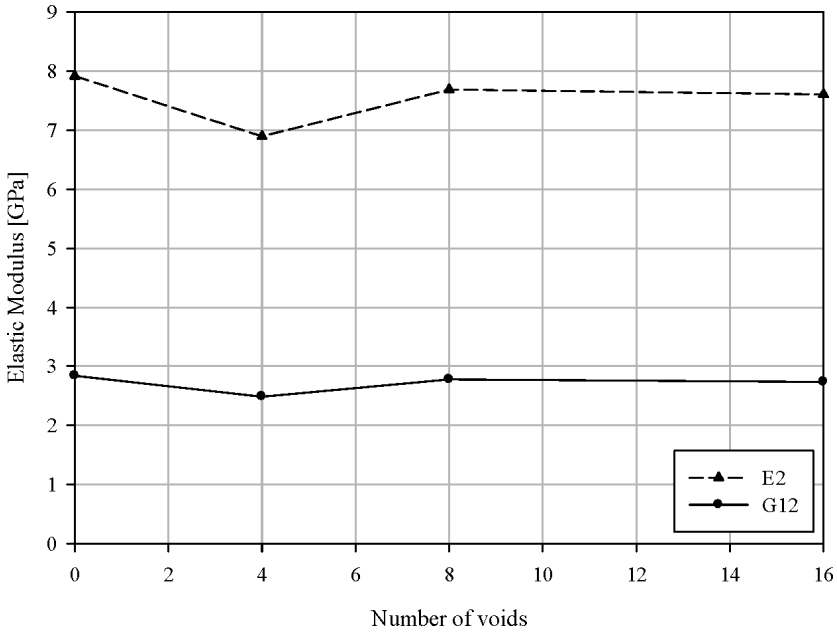

Figure 10 Sensitivity of elastic modulus with void to fibre diameter ratio

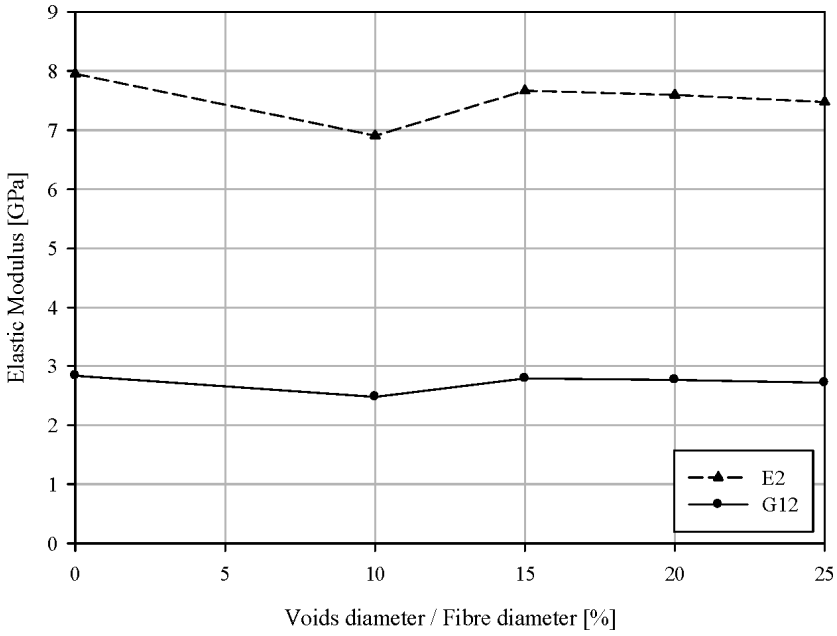

The reasons why the modulus values do not change much may be appreciated by examining the stress contours in Figures 5–8. In all these figures, the stress contours show that a void at an interface introduces a stress concentration problem. Under elastic conditions, stress concentrations induce stress redistributions in an area larger than the area of high gradient, so that the total load is equilibrated. Thus, average values of stress σ and strain ε remain the same in the UC, and their relations, as reflected by elastic modulus, are not affected by the localised concentration of von Mises stress. Average values have been computed using element values and element sizes as weighting factors.

4.2 Elastic stresses around a semi-circular void

As proposed by Kaminski (2005), a void in a plane strain model could be represented by a semi-circular bubble at the interface, with its diameter being a fraction of the fibre diameter. Because of the difference in size, the void itself can be studied at a scale which is approximately 1/10 the scale employed in the investigation of a UC. The domain enclosing a void is illustrated in Figure 11, in which, for simplicity, the curvature of the fibre has not been considered in the geometry.

Figure 11 Domain considered for a semi-circular void under uniaxial stress (see online version for colours)

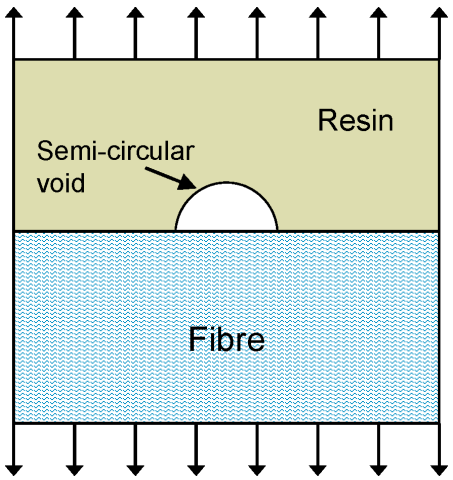

Elastic stress redistributions for this case are shown in Figure 12 for uniaxial and shear loading conditions. For the uniaxial loading case, the base of the void has the highest stresses and the high-stress zones extend in a direction at approximately 45° from the interface (Figure 12(a)). The zone at the centre of the void, on the other hand, takes less load so that overall equilibrium is satisfied.

The stress distributions for a semi-circular void under shear loading was found to produce high stresses in the normal and tangential directions to the fibre, with low values at 45°, as shown in Figure 12(b).

Figure 12 Elastic values of von Mises stress for (a) uniaxial load and (b) shear load (see online version for colours)

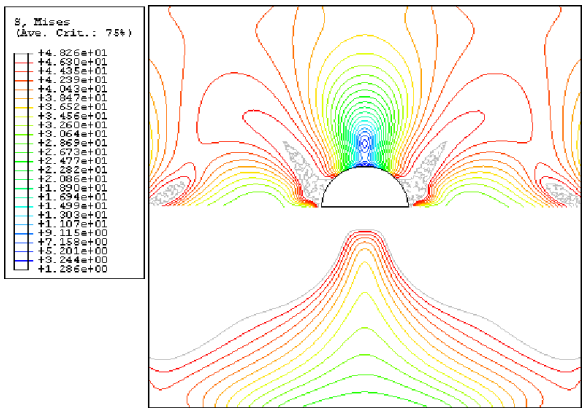

(a)

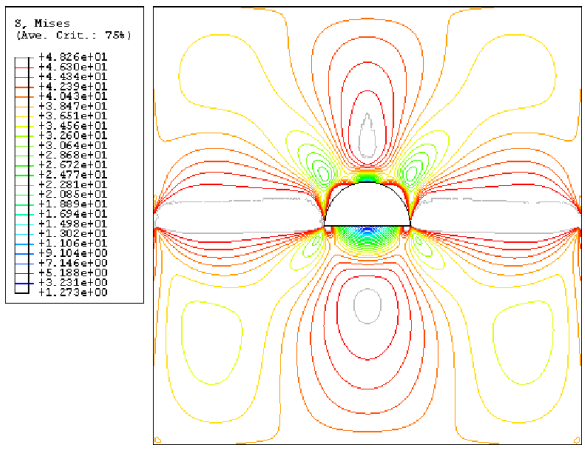

(b)

5 Damage propagation

As discussed in the previous section, damage simulated as interface voids produce stress concentrations affecting the resin matrix. Although the studies reported were carried out for unit stress values at the boundaries of a UC, it is clear that for some values of the applied stress field the matrix reaches its limit strength and damage propagation occurs.

5.1 Damage propagation in the vicinity of a semi-circular void

For more complex problems, such as those occurring at the interface in Figure 13, there are no closed-form analytical solutions and thus have been solved using finite-element analysis with ABAQUS (2003). To represent the results, p is the pressure

acting normal to the fibre–matrix interface, σ_m is the yield stress corresponding to the matrix and r/a is the normalised radial coordinate.

Figure 13 Contour lines enclosing zones of plasticity in a semi-circular void for several levels of (a) uniaxial load and (b) shear load

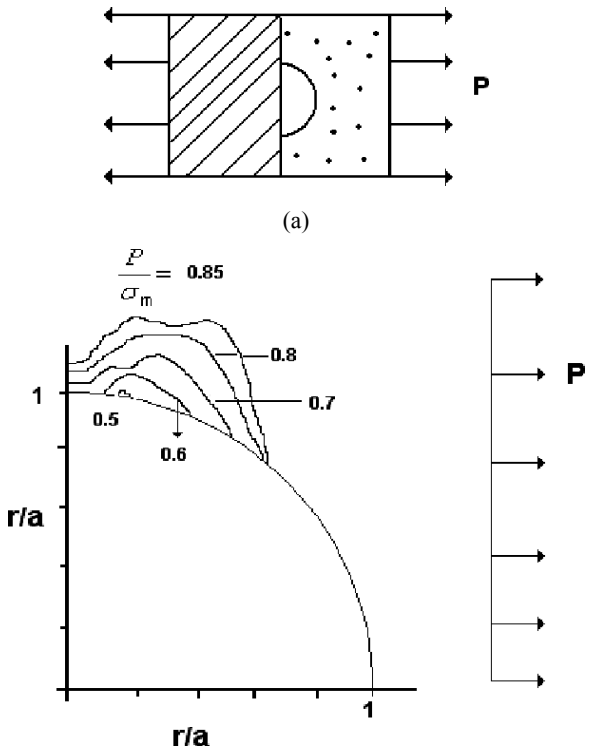

The results of Figure 13 illustrate the extent of the zone affected by plasticity under uniaxial loading. As previously shown in the elastic studies, the zones with high stresses depend on the load considered: the spread of plasticity in the semi-circular void under uniaxial tension is smaller than in the circular void. Under shear, on the other hand, the situation is worse for the semi-circular void and the high stresses affect a zone larger than the diameter of the void for $p/\sigma_m = 0.45$.

5.2 Damage propagation in the vicinity of a semi-elliptical void

The available empirical evidence, such as that shown in the images in Figure 1, indicates that hygro-thermal ageing introduces interface damage that is better represented as a semi-ellipse void, rather than as a semi-circular void. For a specific semi-ellipse with aspect ratio of three, i.e., an ellipse with a ratio of three between its radii, the results for uniaxial and shear stress fields are shown in Figure 14. Again, the uniaxial stress field produces damage extension in a comparatively smaller zone than in the case of shear loading. Similar to what was noticed for the semi-circular void case, for $p/\sigma_m = 0.40$ the damaged zone is larger than the area of original damage due to hygro-thermal ageing.

The effect of this configuration would be to propagate debonding at the interface, so that a larger ellipse (or an interface crack) would be effectively present.

Figure 14 Contour lines enclosing zones of plasticity in a semi-elliptical void for several levels of (a) uniaxial load and (b) shear load

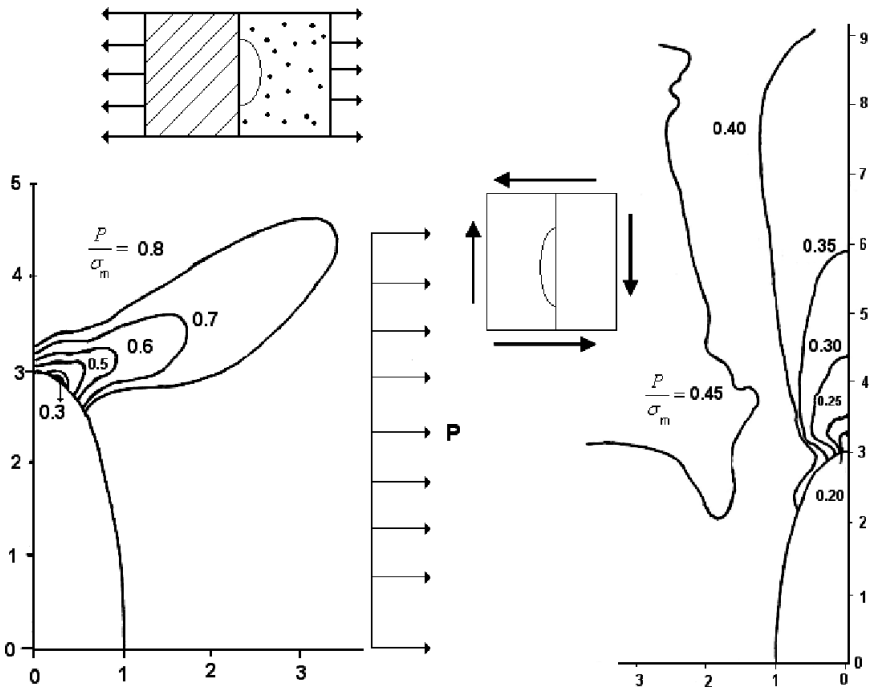

(a) (b)

6 Changes in the GFRP composite stiffness and strength at unit cell level

A constitutive non-linear analysis was used in this section to represent degradation of material properties at a UC level. Specifically, ideal plasticity with the von Mises yield criterion was used to represent the damage threshold in the matrix. The general purpose code ABAQUS (2003) was used to compute the non-linear analysis, using a Newton–Raphson algorithm to follow the nonlinearity of the response.

6.1 Semi-circular voids

Three fibre volume fractions were considered, namely $V_f = 0.3$, 0.5 and 0.7, together with the increasing number of voids and void diameters. Only results for shear loads are shown next, since they produce the highest changes in modulus and strength.

Average values of von Mises stress and strain in a UC are plotted in Figure 15 for different values of V_f. Notably, for a given fibre volume fraction, the curves under different assumed damage conditions show the same elastic modulus. Differences are observed in the non-linear parts of the curve, in which all curves tend to different plateau values which depend on the applied shear level. Also of interest is the maximum strain at

failure, which based on the analyses show dependency with the fibre volume fraction. Failure has been defined in this work as the last value for which the model was able to find an equilibrium configuration. This figure shows that for all V_f values considered the shear strength decreases with increasing void size.

To visualise changes in strength at the UC level, the maximum shear load reached under a given damage condition has been plotted for different void sizes in Figure 16. There is an almost linear sensitivity for $V_f = 0.3$ or 0.5, whereas a more pronounced variation is obtained for $V_f = 0.7$.

Figure 15 Average values of von Mises stress and strain in a UC, for different fibre volume fractions: (a) $V_f = 0.3$; (b) $V_f = 0.5$ and (c) $V_f = 0.7$ (see online version for colours)

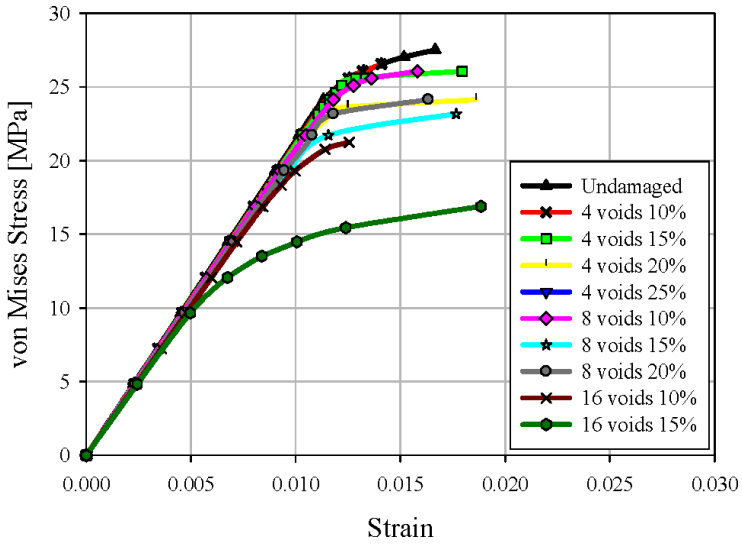

(a)

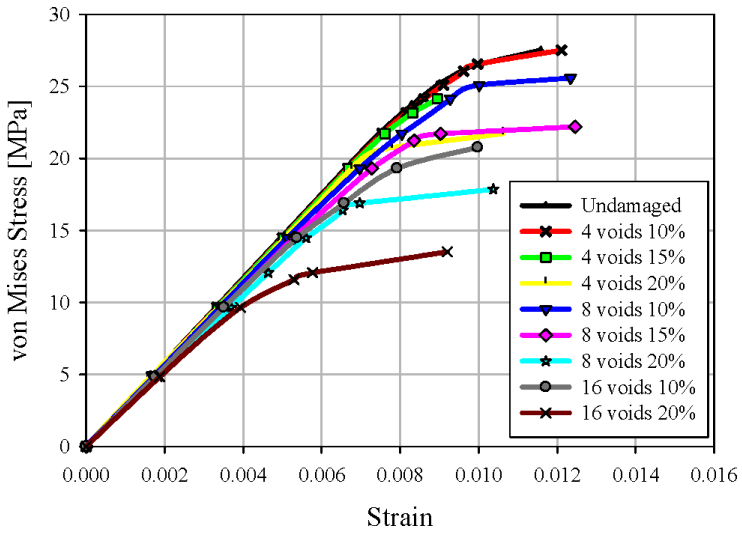

(b)

Figure 15 Average values of von Mises stress and strain in a UC, for different fibre volume fractions: (a) $V_f = 0.3$; (b) $V_f = 0.5$ and (c) $V_f = 0.7$ (see online version for colours) (continued)

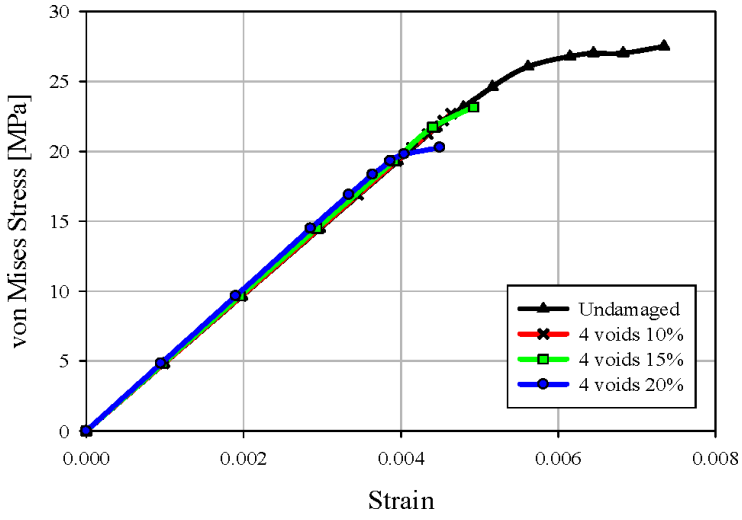

(c)

Figure 16 Sensitivity of shear stress to void to fibre ratio (see online version for colours)

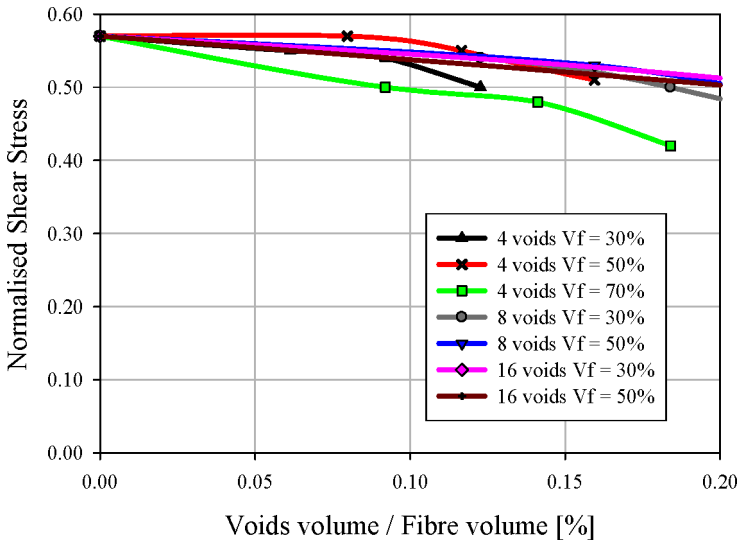

Maximum shear has been normalised with respect to the strength of epoxy.

6.2 Semi-elliptical voids

As discussed earlier, a more realistic consequence of ageing may be obtained by use of semi-elliptical voids at the interface. An example of a UC domain under shear load is shown in Figure 17. The perimeter of the ellipse was taken as a parameter in the study,

with values of 25, 50 and 75% of the perimeter of the fibre. For fibre volume fractions of $V_f = 0.3$ and 0.5, Figure 18 shows shear stress–strain curves similar to those of Figure 15 which were computed for semi-circular voids. Only for the short length debonding case there was a significant deformation before failure, but for the other length cases the loss of elasticity was coincident with failure at the UC level. A summary of sensitivity of the shear strength vs. the length of the interface void is shown in Figure 19. Unlike the case of semi-circular voids, the drop in shear strength depends on the fibre volume fraction, with GFRP composites with high V_f experimenting larger strength reductions.

Figure 17 UC with semi-elliptical void under shear loading (see online version for colours)

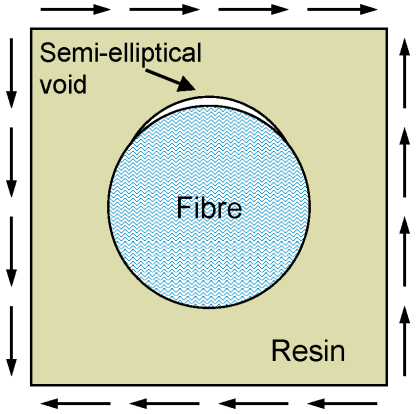

Figure 18 Shear stress vs. strain in UC with semi-elliptical void. (a) $V_f = 0.3$ and (b) $V_f = 0.5$ (see online version for colours)

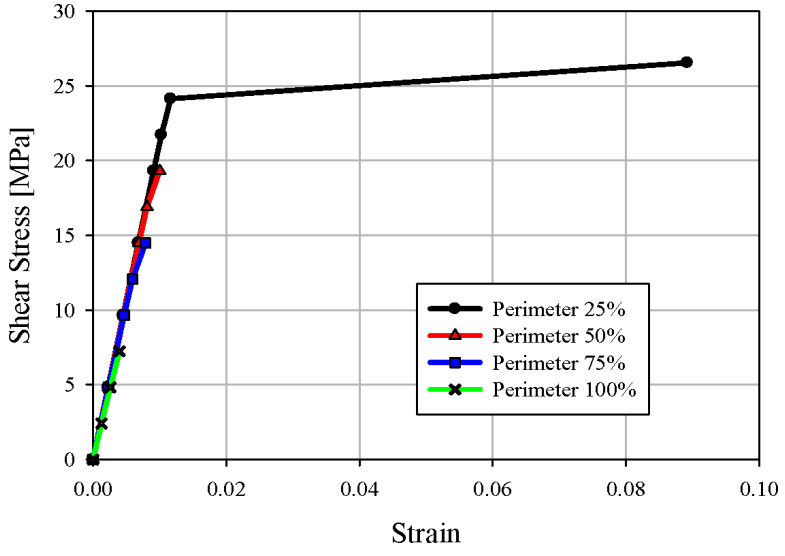

(a)

Figure 18 Shear stress vs. strain in UC with semi-elliptical void. (a) $V_f = 0.3$ and (b) $V_f = 0.5$ (see online version for colours) (continued)

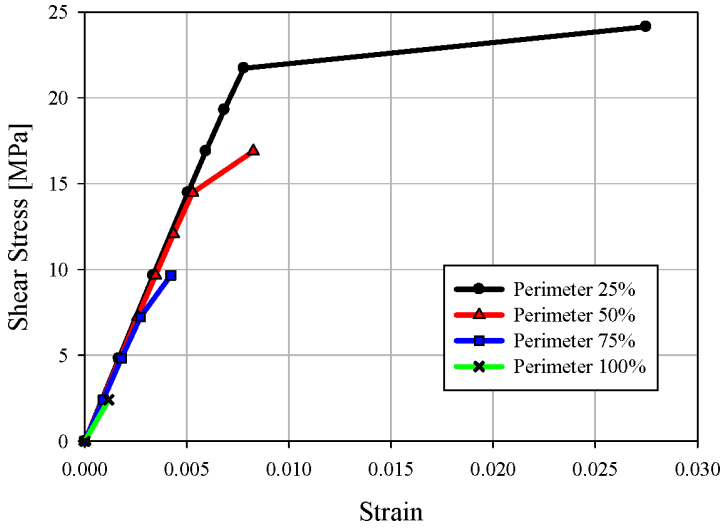

(b)

Figure 19 Sensitivity of shear strength with damage as reflected by the length of interface elliptical void (see online version for colours)

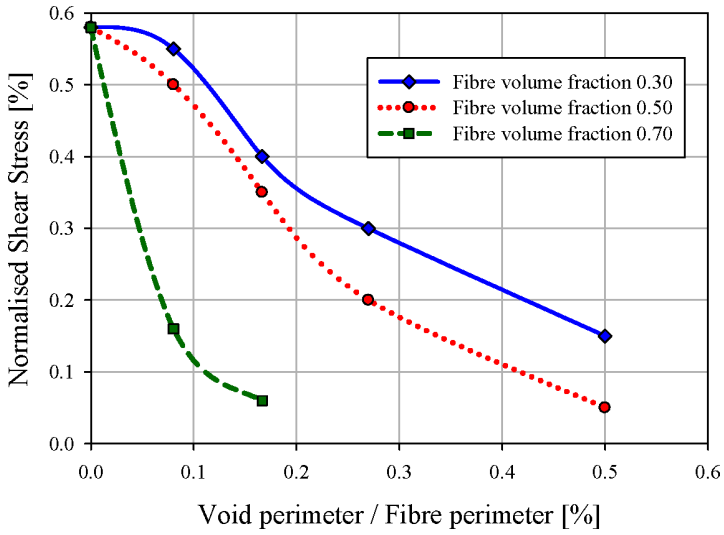

7 Conclusions

The computational studies presented in this paper were based on the simple damage models due to hygro-thermal ageing, in which voids were introduced at the interface and the loads were increased to investigate elastic stress redistributions and damage extension. There are several limitations in the present study:

- the link between ageing time and damage characteristics, as represented by voids, has not been obtained at present in this or other studies reported in the literature
- a two-dimensional (rather than three-dimensional) domain has been used
- micro–macro coupling was not implemented
- fibre damage was not considered.

But even within these limitations, several conclusions may be drawn, as follows.

First, semi-circular voids produce stress concentrations that only affect the neighbourhood of the void. For voids separated between two or three times their diameters, no significant interaction occurs between the zones of modified stress fields and each void can be considered in isolation from their neighbours.

Second, stress concentrations may lead to matrix damage in the area of a void, with the consequence that it produces an effective extension of the damage zone for subsequent load increments. Although actual mechanisms of plasticity in epoxy are not known at the micron level, it seems reasonable to assume that such damage extension will occur for values close to the onset of damage in the matrix.

Third, the situation described so far is aggravated as semi-elliptical (rather than semi-circular) voids are considered at the interface. Damage extension occurs at lower stress levels and affects larger zones in the neighbourhood of a void. Since this is the type of damage that is most commonly observed in SEM images of aged specimens, it is expected that damage will propagate and thus contribute to reduce the strength at a local level.

Fourth, the perplexing behaviour of tests carried out at the macro level, in which the strength is reduced by ageing but the elastic modulus is not significantly affected, can be reinterpreted in view of the present results. For relatively small stress values the material remains elastic and it was seen that only elastic stress redistributions occur, so that stresses are relocated but still have the same average values at UC level. Thus, it is reasonable to observe minor changes in elastic modulus at the micro and macro levels. Damage propagation seems to occur when the threshold of epoxy damage is reached, especially for semi-elliptical voids. This effect would contribute to reduce the strength at local and global levels.

Acknowledgements

The authors gratefully acknowledge the funding received for this project through ARO-DoD Grant No. ARO 51936-EV-H (Program Officer: Dr. Larry Russell). However, the results and opinions expressed are solely of the authors and do not necessarily reflect the views of the funding agency.

References

ABAQUS (2003) *User's Manuals, Version 6.4*, Hibbitt, Karlsson and Sorensen Inc., Rhode Island.

ASTM (2008) *Test Method for Tensile Properties of Polymer Matrix Composite Materials*, Standard D3039, ASTM, West Conshohocken, Pennsylvania.

Barbero, E.J. (2010) *Introduction to Composite Materials Design*, 2nd ed., CRC Press, Boca Raton, FL.

Bonora, N. and Ruggiero, A. (2005) 'Micromechanical modeling of composites with mechanical interface – Part II: damage mechanics assessment', *Composites Science and Technology*, Vol. 66, No. 2, pp.324–332.

Budiansky, B., Evans, A.G. and Hutchinson, J.W. (1995) 'Fiber-matrix debonding effects on cracking in aligned fiber ceramic composites', *Int. J. Solids Structures*, Vol. 32, pp.315–328.

Caporale, A., Luciano, R. and Sacco, E. (2006) 'Micromechanical analysis of interfacial debonding in unidirectional fiber-reinforced composites', *Computers and Structures*, Vol. 84, No. 31, pp.2201–2210.

Car, E., Zalamea, F., Oller, S., Miquel, J. and Oñate, E. (2002) 'Numerical simulation of fiber reinforced composite materials – two procedures', *International Journal of Solids and Structures*, Vol. 39, No. 7, pp.1967–1986.

Cervenka, A., Young, R. and Kueseng, K. (2004) 'Micromechanical phenomena during hygrothermal ageing composites investigated by Raman spectroscopy', *Composites: Applied Science and Manufacturing*, Vol. 36, No. 7, pp.1011–1019.

Davies, P., Pomies, F. and Carlsson, L.A. (1996) 'Influence of water absorption on transverse tensile properties and shear fracture toughness of glass/polypropylene', *Journal of Composite Materials*, Vol. 30, No. 9, pp.1004–1019.

Foulc, M.P., Bergeret, A., Ferry, L., Lenny, P. and Crespy, A. (2005) 'Study of hygrothermal ageing of glass fiber reinforced PET composites', *Polymer Degradation and Stability*, Vol. 89, No. 3, pp.462–469.

He, M.Y., Wu, B.X., Evans, A.G. and Hutchinson, J.W. (1994) 'Inelastic strains due to matrix cracking in unidirectional fiber-reinforced composites', *Mechanics of Materials*, Vol. 18, pp.213–229.

Helbling, C. and Karbhari, V.M. (2005) 'Durability assessment of combined environmental exposure and bending', in Shield, C.K., Busel, J.P., Walkup, S.L. and Gremel, D.D. (Eds.): *Proceedings of the 7th International Symposium Fiber-Reinforced Polymer (FRP) Reinforcement for Concrete Structure*, ACI, SP-230, Farmington Hills, MI, pp.1397–1418.

Kachanov, M. (1986) *Introduction to Continuum Damage Mechanics*, Martinus Nijhoff (Kluwer), Dordrecht.

Kajorncheappunngam, S., Rakesh, K.G. and GangaRao, H.V. (2002) 'Effect of ageing environment on degradation of glass-reinforced epoxy', *Journal Composites of Construction*, Vol. 6, No. 1, pp.61–69.

Kaminski, M. (2005) *Computational Mechanics of Composites Materials*, Springer-Verlag, London.

Lemaitre, J.P. and Desmorat, R. (2010) *Engineering Damage Mechanics*, Springer-Verlag, Berlin.

Lemaitre, J.P. and Krajcinovic, D. (1988) *Continuum Damage Mechanics*, CISM (Int. Center for Mechanical Sciences), Udine, Italy.

McBagonluri, F., Garcia, K., Hayes, M., Verghese, K.N.E. and Lesko, J.J. (2000) 'Characterization of fatigue and combined environment on durability performance of glass-vinyl ester composite for infrastructure applications', *International Journal Fatigue*, Vol. 22, No. 1, pp.53–64.

Sanchez-Palencia, E. and Zaoui, A. (Eds.) (1987) *Homogenization Techniques for Composite Media*, Springer-Verlag, Berlin.

Shutte, C.L. (1994) 'Environmental durability of glass-fiber composites', *Materials Science and Engineering*, Vol. R13, pp.265–324.

Zhang, J.S., Karbhari, V.M., Isley, F. and Neuner, J. (2003) 'Fiber-sizing-based enhancement of materials durability for seismic retrofit', *Journal of Composites for Construction*, Vol. 7, No. 3, pp.194–199.